

SUPPLEMENTAL DATA

Erythroid/megakaryocytic differentiation confers BCL-XL dependency and venetoclax resistance in acute myeloid leukemia

SUPPLEMENTAL NOTE

Clinical description of patients with erythroid/megakaryocytic differentiation

AML-1: Male patient with a history of mild bone marrow (BM) hypoplasia, macrocytosis, and peripheral blood cytopenias (at least) since the age of 31. No routine hematological follow-up until diagnosis of MDS-EB2 at the age of 37 when suffering from severe pancytopenia. Despite therapy (5-azacitidine; 5-azacitidine+venetoclax; chemotherapy with cytarabine and idarubicin) the disease progressed within months. At the study sampling (after progression) the trephine BM biopsy histology demonstrated variable megakaryocytic morphology, with blasts over 20% of the hypercellular BM and 25 % blasts in the peripheral blood. Megakaryocytes were small and hyposegmented. Peripheral blood blasts expressed e.g. CD34/CD42b/CD61/CD33 by flow cytometry. At the study sampling the BM also showed grade 3/3 reticulin fibers. Sampling for drug sensitivity profiling and scRNA-seq were performed on different days, with drug sensitivity profiling performed first and scRNA-seq a week thereafter with no treatment administered during this time.

AML-2: Previously healthy male. T-ALL diagnosed and treated with chemotherapy 5 years preceding MDS with excess of blasts at the age of 41. Therapy-related myeloid malignancy was treated with chemotherapy followed by an allogeneic hematopoietic stem cell transplantation (HSCT) from a registry donor. Relapse occurred 6 months post-HSCT and was treated with 5-azacitidine until progression. At diagnosis and sampling the BM cellularity consisted of only strongly proliferative and dysplastic megakaryocytes and megakaryoblasts. Flow cytometric data from this time point is not available.

AML-3: Female patient. Mastectomy and adjuvant chemotherapy (CEF x6) due to breast cancer 14 years preceding the diagnosis of t-AML at the age of 58. At AML diagnosis and sampling the BM morphology showed remarkable erythroid proliferation (50-60% of the BM cellularity) with dysplasia and an excess of blasts (50% counted from non-erythroid cells). The blasts were positive for CD34/CD117/CD13/CD33/CD11a/CD99/CD133/CD38/CD42a/CD71 (dim)/MPO.

AML-4: Previously healthy 64-year-old male. At diagnosis of AML (and sampling) BM consisted of erythroid proliferation covering 50% of the cellularity with an excess of myeloid blasts (50% counted from all nucleated cells). No dysplasia was detected, due to which a morphologic diagnosis of FAB AML M2 instead of AML NOS erythroid/myeloid was given. Blasts were CD34+/CD117+/CD13+/CD33+/CD99+/CD11a+/CD133+/CD38+. Additionally to a somatic *DDX41* mutation also a germline *DDX41* mutation was detected.¹ Germline *DDX41*-triggered acute leukemias are reported to carry an increased risk for erythroid features.²

AML-5: The patient was diagnosed with essential thrombocythemia at the age of 58. He was treated with aspirin and hydroxyurea. At the age of 71, a BM aspiration was performed due to anemia and leukopenia. He was diagnosed with acute erythroid leukemia. *TP53*, *JAK2* and *ASXL1* mutations were detected, and karyotype was complex. He received one cycle of azacitidine therapy but deceased due difficult infection <30 days from diagnosis.

AML-6: 73 yo female with a previous diagnosis of multiple myeloma. Was treated with several lines of therapy. The diagnosis of therapy-related acute megakaryoblastic leukemia came 3 years later, with monosomy 7 and mutations in *ASXL1* and *KRAS* with 50% blasts. Primary refractory to HMA/venetoclax therapy.

AML-7: 33 yo male patient with relapsed/refractory AML-M6 with complex cytogenetics and *STAG2* mutation, primary refractory to hypomethylating agent (HMA)/venetoclax and intensive chemotherapy/venetoclax therapies.

AML-8: 54 yo female patient with relapsed/refractory AML-M6 with complex cytogenetics and *TP53* mutation, primary refractory to HMA/venetoclax therapy.

SUPPLEMENTAL METHODS

Cell lines

The following 21 AML cell lines were obtained from Deutsche Sammlung von Mikroorganismen und Zellkulturen (DSMZ). FAB M2 (KASUMI1, SH-2, and HL60), FAB M3 (PL-21), FAB M4 (OCI-AML2, GDM-1, HNT-34, and ML-2), FAB M5 (SKM-1, SHI-1, THP-1, MV4-11, NOMO-1, and MOLM13), FAB M6 (F-36P, OCI-M1, TF-1, HEL, and KG-1), and FAB M7 (M-07e and CMK). More specific cell line information and culture conditions can be found from supplemental Table 1. All assays were performed with cells from early passages and cell lines were cultured for 3-5 days after thawing to obtain steady growth before performing the assays. The 293FT cell line used for lentivirus production was obtained from Thermo Fisher Scientific and cultured in DMEM (Lonza) with 10% FBS, 2 mM L-glutamine, 100 U/mL penicillin, and 100 µg/mL streptomycin (Gibco) (D10).

Processing and culture of patient samples

BM or peripheral blood (PB) samples were enriched for mononuclear cells (MNCs) using Ficoll gradient centrifugation. Thawed samples were resuspended in 87.5% RPMI1640 medium plus 12.5% HS-5 stromal cell conditioned medium (CM),³ supplemented with 10% FBS, L-glutamine (2 mM) and penicillin/streptomycin (100 units/ml). After thawing, all samples were treated with 50 µl of RQ1 RNase-Free DNase (Promega, #M6101) for 30 min in 1 ml of CM. Samples were recovered for 4 h in 10 ml of CM before plating on drug plates. Freshly isolated MNCs of the two index cases (AML-1 and AML_5) were used in flow cytometry-based drug sensitivity profiling. Patient characteristics are presented in supplemental Table 1.

Drug sensitivity profiling

384-well drug plates were prepared by the FIMM High Throughput Biomedicine Unit. Cell lines were seeded on the drug plates at a cell line-specific cell density and culture medium (supplemental Table 1). Ficoll-purified mononuclear cells of primary patient samples were seeded on BCL-2 family-specific drug plates in conditioned medium

(CM) at a cell density of 7,500–10,000 cells per well. All cells were incubated with the drugs for 72 h at 37°C and 5% CO₂ and viabilities were assessed using the CellTiter-Glo assay (Promega). The luminescence signal was measured using a PHERAstar plate reader (BMG Labtech). Differences in drug sensitivity between erythroid/megakaryoblastic and other AML cell lines were assessed using Welch's *t*-test on the DSS values followed by Benjamini-Hochberg adjustment of *P* values.

Genome-wide CRISPR and RNAi screen data analysis

Genome-wide CRISPR screen data from the DepMap project were downloaded from the DepMap portal (<https://depmap.org/portal/download/>) as CERES-corrected gene effect values⁴ (CRISPR Avana Public 20Q2 dated 05/2020, 'Achilles_gene_effect.csv') together with cell line annotations ('sample_info.csv'). RNAi screening data from the Achilles project were downloaded from the DepMap portal (<https://depmap.org/portal/download/>) as DEMETER-inferred gene knockdown effects (Achilles 2.20.2 dated 07/2017, 'portal-RNAi_merged-2018-06-21.csv').⁵ Differences in gene essentiality between erythroid/megakaryocytic leukemia and other AML cell lines were assessed using Welch's *t*-test on the gene effect values followed by Benjamini-Hochberg adjustment of *P* values and the differential gene effect was calculated by subtracting the average gene effect of erythroid/megakaryoblastic cell lines from that of the other cell lines.

Analysis of genome-wide CRISPR screen data from Wang et al.

Genome-wide CRISPR screen data as CRISPR scores were obtained from supplementary material of Wang et al.⁶ Genes were ranked by subtracting the average CRISPR score of the erythroid cell lines from that of the other AML cell lines.

Western blot analysis

Three million cells from each cell line were spun down (500 x g for 5 min) and washed with ice-cold PBS. Cell pellets were lysed in 100 µl RIPA (Cell Signaling Technology, #9806) supplemented with 1 mM PMSF. After 30 min incubation on ice, samples were centrifuged at 15,000 x g for 15 min at 4°C and supernatants were transferred to new Eppendorf tubes. Protein concentration was quantified using the Qubit protein assay kit (ThermoFischer Scientific, Q33212) and 30 µg of protein was loaded onto 12% SDS-PAGE gels (Bio-Rad). Following electrophoresis (100V) the proteins were

transferred onto nitrocellulose membranes (Bio-Rad, 0.2 μm , #162-0112) and blocked with 5% bovine serum albumin (BSA) dissolved in Tris-buffered saline (TBS) for 1h. Primary antibodies were obtained from Cell Signaling Technology; anti-BCL-2 (cat. 4223) anti-MCL-1 (cat. 5453), anti-BCL-XL (cat. 2764) and loading control antibody from Sigma-Aldrich, anti- β -actin (cat. 20-33). Primary antibodies were diluted in TBS + 5% BSA + 0.05% Tween 20 (TBS-T) in 1:1000 dilution and incubated with the membranes for 2 h at room temperature (RT). Secondary infrared antibodies IRDye 800CW (926-32211, rabbit) and IRdye680RD (cat. 926-68070, mouse) from LI-COR Biosciences were diluted 1:15,000 in TBS-T + 5% BSA, and incubated with the membranes for 1 h at RT. Membranes were washed three times with TBS after which they were visualized with the Odyssey imaging system (LI-COR Biosciences).

Analysis of the effect of *GFI1B* or *GATA1* knockdown on *BCL2L1* expression

Data from genome-scale Perturb-seq by Replogle et al.⁷ where genes are silenced using CRISPRi in the K562 erythroleukemia cell line were downloaded from FigShare (<https://doi.org/10.25452/figshare.plus.20029387.v1>). The gemgroup Z-normalized pseudo-bulk expression data for genes expressed at >0.01 UMI per cell from the genome-wide screen in K562 were used for the analysis. All measured genes were ranked based on the Z-scores in the *GFI1B* and *GATA1* knockdown groups to determine the ranks and Z-scores of the genes of interest *BCL2L1* and *GYP A* (encoding the erythroid differentiation marker glycoporphin A as a reference).

CRISPR-Cas9-mediated *TP53* knockout

Constructs encoding a single-guide RNA (sgRNA) targeting *TP53* (GGCAGCTACGGTTTCCGTC)⁸ and a control sgRNA targeting a safe genomic region (GGGTAGAATACCCCATT)⁹ were cloned into lentiCRISPRv2 (a gift from Feng Zhang, Addgene # 52961). To produce lentivirus, 293FT cells were seeded at 3.8 million cells in a T-75 flask and on the next day 20 μg of the lentiCRISPRv2 plasmid was transfected with 7.5 μg of psPAX2 (a gift from Didier Trono, Addgene plasmid # 12260) and 2.5 μg of pCMV-VSV-G (a gift from Bob Weinberg, Addgene plasmid # 8454) using 40 μl Lipofectamine 2000 (Thermo Fisher Scientific) according to the manufacturer's instructions. After 6 h, the culture medium was replaced with D10 containing 1% BSA. After 60 h, viral supernatant was harvested, filtered using a 0.45 μm filter, concentrated by overnight centrifugation at 5,000 g, and stored in -70°C . To

transduce cells, 500,000 cells of either MOLM13, MV411, or OCIAML2 were suspended in 25 μ l concentrated virus and 225 μ l culture medium with 8 μ g/ml Polybrene in a 24-well plate well, centrifuged at room temperature at 800 g for 2 h, after which virus was washed away. Cells were selected using the MDM2 inhibitor idasanutlin (100 nM) to enrich for cells with functional TP53 inactivation which confers resistance to MDM2 inhibition. Drug sensitivity profiling on the edited cells was performed as described for the other cell lines. DSS values of the *TP53* knockout cell lines were compared with the parental unmodified versions using a paired Welch's *t*-test.

Gene expression analysis

Hemap gene expression data¹⁰ as log₂ expression values (syn21991190) and sample annotations (syn21995216) were downloaded from Synapse (DOI: 10.7303/syn21991014). Differential gene expression analysis between AML M6 samples and all other hematological malignancies was performed using the Wilcoxon rank-sum test followed by Benjamini-Hochberg adjustment of *P* values.

TCGA AML data¹¹ were preprocessed as previously described.¹² The processed feature matrix of multi-omic and clinical data was downloaded from Synapse (DOI: 10.7303/syn21991014, syn21991203). Expression of BCL-2 family genes was plotted using log₂ RSEM values.

CCLE RNA-seq¹³ gene expression and mutation data (05/22) were downloaded from the DepMap portal (<https://depmap.org/portal/download/all/>).

Colony-forming assays

Mononuclear cells of two healthy bone marrow samples were thawed rapidly at +37°C, washed and treated with DNase for 15 min after resuspending in StemSpan SFEMII medium (STEMCELL Technologies). The other sample (shown in Figure 3F) was pretreated with the indicated drugs in a 12-well plate for 24 hours; 1. DMSO (control) 2. A-1331852 (100nM) 3. venetoclax (200nM) and 4. navitoclax (500nM). After 24 hours, cells were calculated and same number of viable cells from each condition was used in the clonogenic assay. For the other sample (shown in supplemental Figure 5), cells were recovered 24 hours in SFEMII after the indicated drugs and cells were

mixed in the semisolid medium. Colony-forming assay were conducted according to manufacturer's instructions using MethoCult™ H4434 Classic Methylcellulose-based medium with recombinant cytokines for human cells (STEMCELL Technologies). 50,000 viable cells were seeded to each well in 6-well plates and after 14 days, colony forming units were calculated using light microscopy. All conditions were tested in triplicates to calculate the mean colony numbers.

Human Cell Atlas data processing

Human Cell Atlas normal BM scRNA-seq data¹⁴ were preprocessed and filtered as previously described.¹⁵ The processed data are available at Synapse (DOI: 10.7303/syn21991014, syn21995190). The R package HGNCHELPER was used for mapping the gene symbols to most recent symbols. R version 3.6 and Seurat R package v3¹⁶ were used for scRNA-seq data analysis. Data normalization was performed using SCTransform with 3,000 variable features. Batch correction between patients was performed using batchelor 1.01 R package tool fastMNN¹⁷. For the UMAP projection, 50 PCs from fastMNN run were used and Louvain's algorithm with resolution set to 0.5 was used for clustering. Automated cell type annotation was performed with the SingleR package (1.0.1)¹⁸ using ENCODE/Blueprint annotations.

Single-cell RNA sequencing

The libraries were sequenced on Illumina NovaSeq 6000 system using read lengths: 28bp (Read 1), 10bp (i7 Index), 10bp (i5 Index) and 90bp (Read 2). Data from samples AML-sc-A, AML-sc-B, and AML-sc-C have been previously published.¹⁵ The Cell Ranger v4.0 (v3.1 for previously published samples) mkfastq and count analysis pipelines (10x Genomics) were used to demultiplex and convert Chromium single-cell sequencing barcode and read data to FASTQ files and to align reads to GRCh38 and generate gene-cell matrices.

R-package Seurat¹⁶ in R and Python library scVI¹⁹ (0.5.0) in Python (3.7.4) were used for scRNA-seq data processing. Cells with > 15% mitochondrial gene counts, > 50% or < 5% ribosomal gene transcripts, less than 1,000 or more than 30,000 UMI counts, or less than 300 or more than 5,000 detected genes were filtered out. For the index cases (AML-1 and AML-5), after log-normalization the highly variable genes were calculated with the VariableFeatures function implemented in Seurat with removing

genes related to V(D)J recombination. The UMAP dimensionality reduction with default parameters was calculated from the principal components with > 2 standard deviations (n = 22). Batch correction for removing technical variation between the profiled patients (AML-1 and AML-5) and the previously published patients was done with the default workflow implemented in scVI with default parameters and the 30 latent dimensions were used for UMAP dimensionality reduction with n.neighbors = 50 and min.dist = 0.5 parameters. R package SingleR¹⁸ (1.0.1) was used for the automated reference-based cell type annotation, using ENCODE/Blueprint annotations available in the package. Differential expression was performed using the FindMarkers function in Seurat with logfc.threshold = 0.1.

Copy-number analysis from single-cell RNA-sequencing data

Copy-number analysis from scRNA-seq data was performed using the inferCNV R package (v1.12.0) of the Trinity CTAT Project. (<https://github.com/broadinstitute/inferCNV>). An InferCNV object was created using the CreateInfercnvObject function using the read count matrix after filtering out low-quality cells, cell type annotations based on SingleR at the level of either single cells (AML-1) or clusters (AML-5), and a gencode_v19 gene order file downloaded from <https://data.broadinstitute.org/Trinity/CTAT/cnv/>. T and NK cells were used as the reference group as these populations are not expected to harbor copy-number alterations found in myeloid malignancies. InferCNV was the run using the run command with cutoff = 0.1.

Flow cytometry-based drug sensitivity profiling

The FIMM High Throughput Biomedicine Unit (HTB) performed flow cytometry-based drug sensitivity profiling for AML-1 patient. Compounds were dissolved in 100% dimethyl sulfoxide and dispensed on a 384-well polypropylene plate (Greiner) in a 7-dose half-log concentration series using an Echo 550 acoustic liquid handling device (Labcyte). PBMC were dispensed with MultiFlow FX.RAD (BioTek) to compound plates, 20,000 live cells in 20 µl CM in each well and incubated for 72 h at 37°C and 5% CO₂. Monoclonal antibodies (BD Biosciences) CD38-BV421 (#562444), CD11b-BV605 (#562721), CD15-BV786 (#741013), CD34-PE (#550761), CD45-V500 (#560777), CD14-APC (#555399), CD117-PE-Cy7 (#313212), apoptosis dye Annexin-V-FITC (#556419), and dead cell exclusion dye DRAQ7 (Cell Signaling

Technologies, #7406) were added on cells with Echo 525 (Labcyte Inc.) and stained for 30 min at room temperature. Cells were analyzed with iQue Screener Plus flow cytometer (Intellicyt). For AML-5 patient, flow cytometry-based drug sensitivity profiling was performed similarly as described by Kuusanmäki et al.²⁰ with a few modifications. Following a 48-hour incubation, cells were stained with an antibody mix containing CD45, CD34, CD117, CD14, CD11b, CD64, and CD38, followed by apoptosis (Annexin V) and dead cell staining (7-AAD).

Remaining live single cells after drug treatment were gated using FlowJo (Treestar) (supplemental Figure 10A) and unsupervised clustering was performed using the cluster function in the CATALYST R package relying on FlowSOM²¹ and ConsensusClusterPlus²² using maxK = 20. Clusters representing > 5% cells were annotated based on marker expression and remaining cells were annotated as 'Other'. UMAP dimensionality reduction was performed using the runDR command in CATALYST by downsampling the cells to 1,000 per well.

Generation of luciferase-expressing HEL cell line

The HEL erythroleukemia cell line was transduced with LV-SFFV-Luc2-P2A-EmGFP lentivirus obtained from Imanis Life Sciences (Rochester, Minnesota, USA). First, 20,000 cells were resuspended to 50 µl of cell culture medium and plated on a well on a 96-well plate and 50 µl of virus suspension and 0.1 µl of Polybrene were added. Cells were then centrifuged for 2 hours at 800 g, after which the supernatant was removed and the cells were resuspended in 100 µl of fresh medium. Cells were selected using 1 µg/ml puromycin for 13 days and single GFP-bright cells were sorted with a Sony SH800 cell sorter to 96-well plates and expanded for 3 weeks. The brightest GFP-positive clone was chosen for the mouse experiments.

Formulation of oral A-1331852

A-1331852 used in the animal studies was obtained from Chemietek. For oral administration, the suspension was prepared as described by Levenson et al.²³ First, A-1331852 was suspended in DMSO (100 mg/ml) and aliquoted in -80°C to prepare fresh solution every 2-3 days. Upon thawing A-1331852 was suspended to ethanol until a uniform cloudy suspension was achieved. Phosal 50 PG and PEG 400 were then added and the solution was vortexed. Final solution contained 60% Phosal 50

PG, 27.5 % PEG 400, 10% ethanol, and 2.5 % DMSO. A water bath sonicator was also used for 5 min. Formulated solution was stored in +4°C in a tube covered with aluminium foil and used for 2-3 days for oral administration.

Mouse xenograft experiments

Thirty female NOD/SCID mice (NOD.CB-17-Prkdc scid/Rj) were obtained from Janvier Labs (Le Genest, Pays de la Loire, France). Mice were housed in the HiLIFE Laboratory Animal Centre of the University of Helsinki. All procedures were approved by the national Project Authorisation Board, protocol ESAVI 691. Four mice were housed per IVC-cage and food and water were freely available. Mice were acclimatized to the animal facilities for 10 days before start of the experiments.

Four million HEL erythroleukemia cells expressing luciferase were injected intravenously into NOD/SCID mice. After 24 days from injection 11 out of 30 mice harbored detectable tumors. Mice were size-matched based on tumor burden and divided to control (n=5) and treatment group (n=6). Mice were treated twice a day orally with BCL-XL inhibitor A-1331852 (25 mg/kg, 200 µl suspension) or vehicle control for two weeks. Tumor sizes were measured twice per week by injecting 100 µl D-luciferin intraperitoneally under isoflurane anesthesia and imaging the dorsal and ventral sides of each animal after a 20-minute wait on Lago (Spectral Instruments, AZ, United States). Animals were monitored daily for clinical symptoms and weight loss; a health scoring system was used to determine the humane endpoint.

Combination screens

Erythroid (OCIM1, HEL, F36P) and megakaryoblastic (M07, TF1, CMK) leukemia cell lines were plated to 384-well drug combination plates containing five 8x8 combination matrixes. Each matrix was comprised of seven different concentrations of each drug and a DMSO control well. After 72 hours, cell viability was measured using the CTG reagent as described in the drug sensitivity profiling section. Seeding density and used medium for each cell line are presented in supplementary Table 1.

Synergy, efficacy, and integrated synergy and efficacy scores (STE) were calculated for each drug combination using a web-based tool (<https://syntoxprofiler.fimm.fi>).²⁴ Combination efficacy was quantified based on the normalized volume under dose-

response surface (efficacy volume score). Synergy effect was quantified using the zero-interaction potency (ZIP) model.²⁵ The generated delta score is an average combination effect of the drugs over all the tested concentrations. The delta score >0 implies synergistic and <0 antagonistic effect of drugs. The best drug combinations for each cell line were ranked with the STE score, which integrates combination synergy and efficacy.

Long-term drug combination assays

TF1, CMK, and HEL cell lines were used to assess long term efficacy of A-1331852 (50 nM), venetoclax (300 nM), azacitidine (500 nM), ruxolitinib (300 nM) and A-1331852 combined with the other tested drugs. Used drug concentrations were chosen based on the 3-day drug combination studies. One million cells per treatment were seeded to 6-well plates at 250,000 cells/ml in 4 ml of medium recommended for the used cell lines. Viable cells were calculated every 3-4 days using Countess II Automated Cell Counter (Thermo Fisher Scientific, Waltham, MA) and trypan blue to exclude dead cells. After cell counting, cells were washed, and one million cells (if available) were re-seeded in 4 ml of fresh medium and compounds. When needed, the splitting factor was marked down to estimate the total number of cells during the passages. Cells were treated with the compounds for 3 weeks and subsequently cultured for 2 weeks to measure the recovery of the cells after withdrawing the drugs.

SUPPLEMENTAL REFERENCES

1. Wartiovaara-Kautto U, Hirvonen EAM, Pitkänen E, et al. Germline alterations in a consecutive series of acute myeloid leukemia. *Leukemia*. 2018;32(10):2282–2285.
2. Lewinsohn M, Brown AL, Weinel LM, et al. Novel germ line DDX41 mutations define families with a lower age of MDS/AML onset and lymphoid malignancies. *Blood*. 2016;127(8):1017–1023.
3. Karjalainen R, Pemovska T, Popa M, et al. JAK1/2 and BCL2 inhibitors synergize to counteract bone marrow stromal cell–induced protection of AML. *Blood*. 2017;130(6):789–802.
4. Meyers RM, Bryan JG, McFarland JM, et al. Computational correction of copy number effect improves specificity of CRISPR–Cas9 essentiality screens in

- cancer cells. *Nat. Genet.* 2017;49(12):1779–1784.
5. Tsherniak A, Vazquez F, Montgomery PG, et al. Defining a Cancer Dependency Map. *Cell.* 2017;170(3):564-576.e16.
 6. Wang T, Yu H, Hughes NW, et al. Gene Essentiality Profiling Reveals Gene Networks and Synthetic Lethal Interactions with Oncogenic Ras. *Cell.* 2017;168(5):890-903.e15.
 7. Replogle JM, Saunders RA, Pogson AN, et al. Mapping information-rich genotype-phenotype landscapes with genome-scale Perturb-seq. *Cell.* 2022;185(14):2559-2575.e28.
 8. Drost J, van Jaarsveld RH, Ponsioen B, et al. Sequential cancer mutations in cultured human intestinal stem cells. *Nature.* 2015;521(7550):43–47.
 9. Morgens DW, Wainberg M, Boyle EA, et al. Genome-scale measurement of off-target activity using Cas9 toxicity in high-throughput screens. *Nat. Commun.* 2017;8(1):15178.
 10. Pölönen P, Mehtonen J, Lin J, et al. Hemap: An interactive online resource for characterizing molecular phenotypes across hematologic malignancies. *Cancer Res.* 2019;canres.2970.2018.
 11. Cancer Genome Atlas Research Network; Timothy J Ley, Christopher Miller, Li Ding, Benjamin J Raphael, Andrew J Mungall, A Gordon Robertson KH. Genomic and Epigenomic Landscapes of Adult De Novo Acute Myeloid Leukemia. *N. Engl. J. Med.* 2013;368(22):2059–2074.
 12. Mehtonen J, Pölönen P, Häyrynen S, et al. Data-driven characterization of molecular phenotypes across heterogeneous sample collections. *Nucleic Acids Res.* 2019;47(13):e76–e76.
 13. Ghandi M, Huang FW, Jané-Valbuena J, et al. Next-generation characterization of the Cancer Cell Line Encyclopedia. *Nature.* 2019;569(7757):503–508.
 14. Hay SB, Ferchen K, Chetal K, Grimes HL, Salomonis N. The Human Cell Atlas bone marrow single-cell interactive web portal. *Exp. Hematol.* 2018;68:51–61.
 15. Dufva O, Pölönen P, Brück O, et al. Immunogenomic Landscape of Hematological Malignancies. *Cancer Cell.* 2020;38(3):380-399.e13.
 16. Stuart T, Butler A, Hoffman P, et al. Comprehensive Integration of Single-Cell Data. *Cell.* 2019;177(7):1888-1902.e21.
 17. Haghverdi L, Lun ATL, Morgan MD, Marioni JC. Batch effects in single-cell

- RNA-sequencing data are corrected by matching mutual nearest neighbors. *Nat. Biotechnol.* 2018;36(5):421–427.
18. Aran D, Looney AP, Liu L, et al. Reference-based analysis of lung single-cell sequencing reveals a transitional profibrotic macrophage. *Nat. Immunol.* 2019;20(2):163–172.
 19. Lopez R, Regier J, Cole MB, Jordan MI, Yosef N. Deep generative modeling for single-cell transcriptomics. *Nat. Methods.* 2018;15(12):1053–1058.
 20. Kuusanmäki H, Leppä A-M, Pölönen P, et al. Phenotype-based drug screening reveals association between venetoclax response and differentiation stage in acute myeloid leukemia. *Haematologica.* 2020;105(3):708–720.
 21. Van Gassen S, Callebaut B, Van Helden MJ, et al. FlowSOM: Using self-organizing maps for visualization and interpretation of cytometry data. *Cytom. Part A.* 2015;87(7):636–645.
 22. Wilkerson MD, Hayes DN. ConsensusClusterPlus: a class discovery tool with confidence assessments and item tracking. *Bioinformatics.* 2010;26(12):1572–1573.
 23. Levenson JD, Phillips DC, Mitten MJ, et al. Exploiting selective BCL-2 family inhibitors to dissect cell survival dependencies and define improved strategies for cancer therapy. *Sci. Transl. Med.* 2015;7(279):279ra40.
 24. Ianevski A, Timonen S, Kononov A, Aittokallio T, Giri AK. SynToxProfiler: An interactive analysis of drug combination synergy, toxicity and efficacy. *PLOS Comput. Biol.* 2020;16(2):e1007604.
 25. Yadav B, Wennerberg K, Aittokallio T, Tang J. Searching for Drug Synergy in Complex Dose–Response Landscapes Using an Interaction Potency Model. *Comput. Struct. Biotechnol. J.* 2015;13:504–513.

SUPPLEMENTAL TABLES

Supplemental Table 1. Cell line and patient characteristics.

Supplemental Table 2. Drug sensitivity data of 528 drugs in 9 AML cell lines.

Supplemental Table 3. Drug sensitivity data of BCL-2 family drugs in 21 AML cell lines.

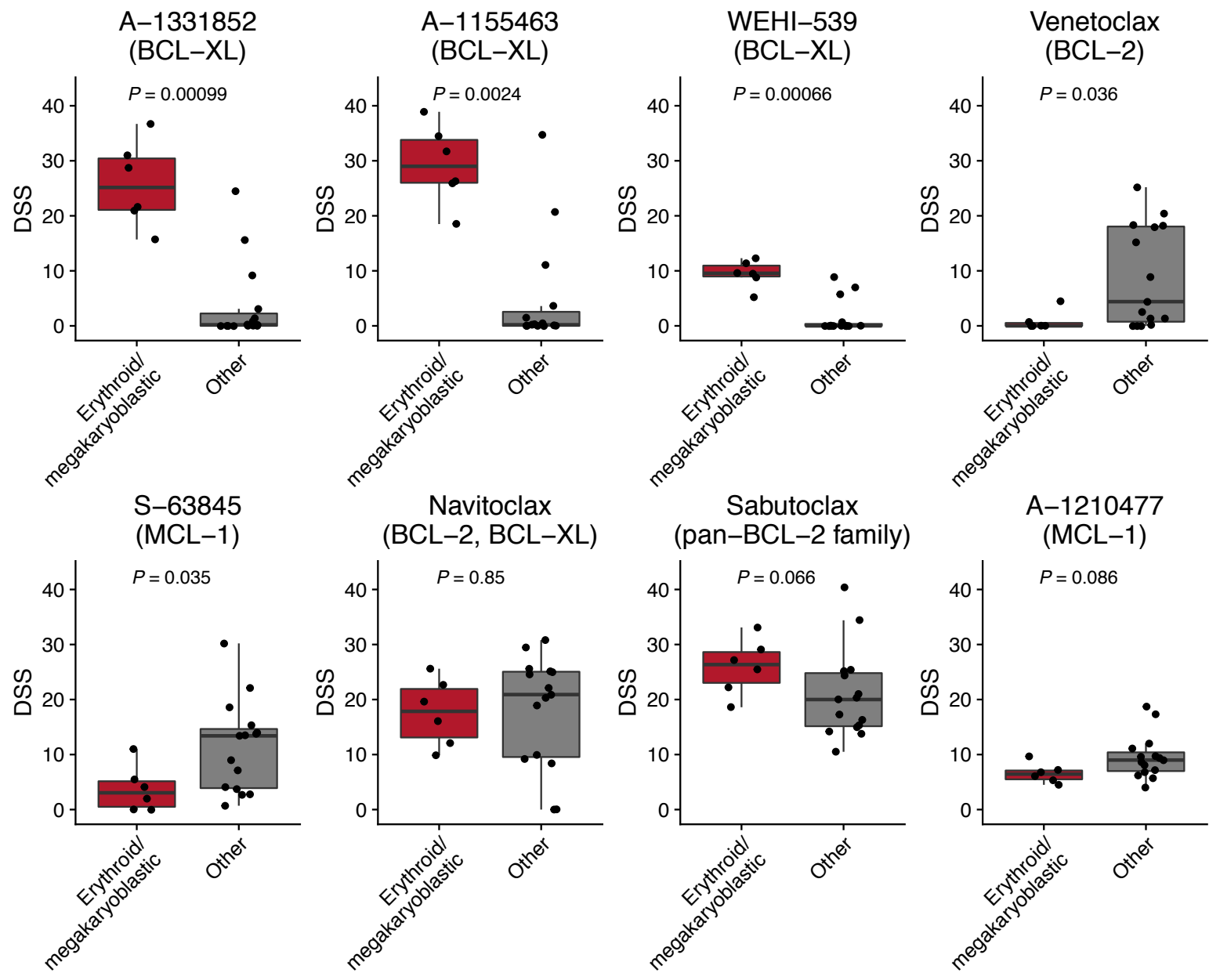
Supplemental Table 4. Differential expression and gene essentiality between erythroid/megakaryoblastic leukemias and other hematological malignancies.

Supplemental Table 5. Differential expression and cell type annotations in scRNA-seq data.

Supplemental Table 6. Drug combination efficacy, synergy, and dose response matrices.

SUPPLEMENTAL FIGURES

Supplemental Figure 1

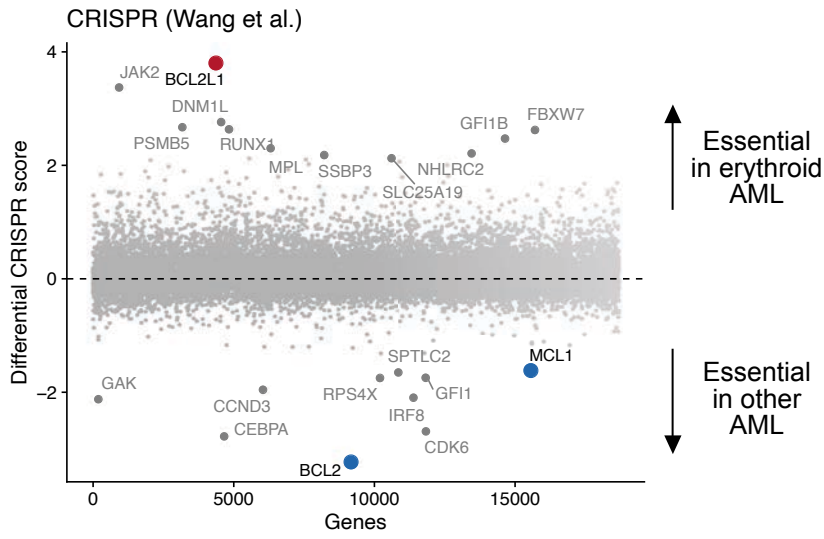


Supplemental Figure 1. Drug sensitivity profiling of drugs targeting BCL2 family proteins in AML cell lines.

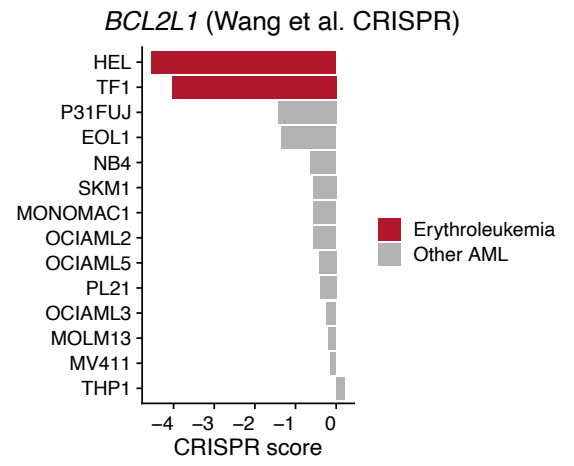
Box plots of drugs targeting BCL-2 family members in erythroid or megakaryoblastic cell lines (n = 6) compared to other AML cell lines (n = 15). DSS values are obtained from optimized area under the dose response curve with higher values indicating higher efficacy. *P* values were obtained using Wilcoxon rank-sum test. In box plots, the horizontal line indicates the median, boxes indicate the interquartile range, and whiskers extend from the hinge to the smallest/largest value, at most 1.5 interquartile range from the hinge.

Supplemental Figure 2

A

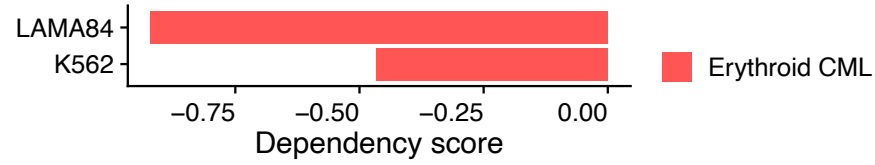


B



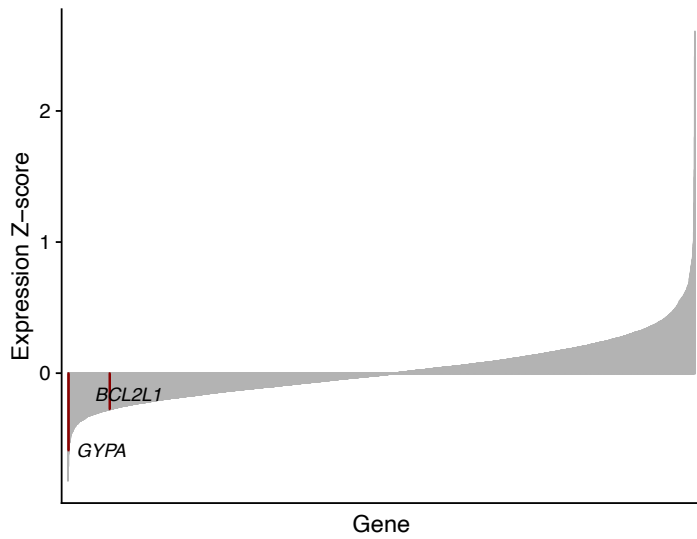
C

BCL2L1 RNAi

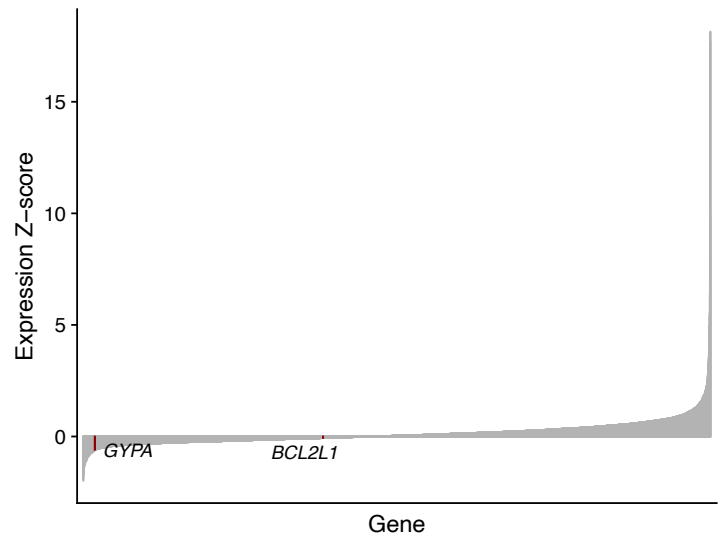


D

GF11B knockdown



GATA1 knockdown



Supplemental Figure 2. Essentiality of *BCL2L1* in erythroid leukemia cell lines in additional CRISPR-Cas9 and RNAi datasets and effects of *GFI1B* and *GATA1* knockdown on *BCL2L1* expression.

(A) Scatter plot of differential CRISPR scores between AML M6 cell lines and other AML in genome-wide CRISPR-Cas9 screening data from Wang et al. Top and bottom 10 genes are labeled and the BCL-2 family genes *BCL2L1*, *BCL2*, and *MCL1* are colored based on the direction of the differential CRISPR score. Genes are ordered by their location on the chromosomes.

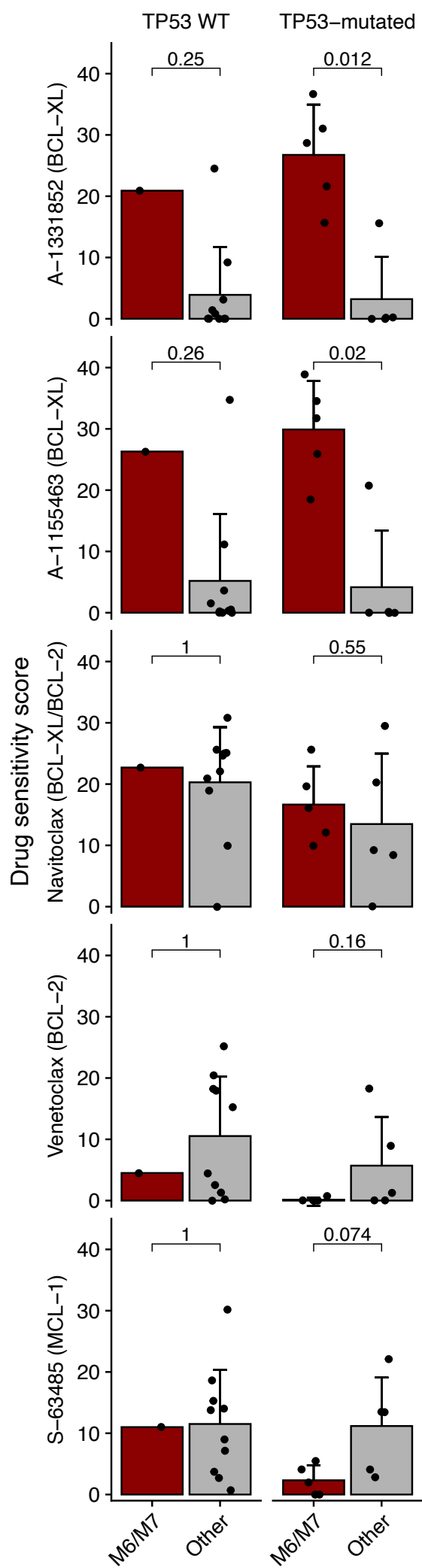
(B) *BCL2L1* CRISPR score in AML cell lines from Wang et al. More negative values indicate stronger dependency.

(C) *BCL2L1* dependency score in erythroid CML cell lines in RNAi screening data from the Achilles project. More negative values indicate stronger dependency.

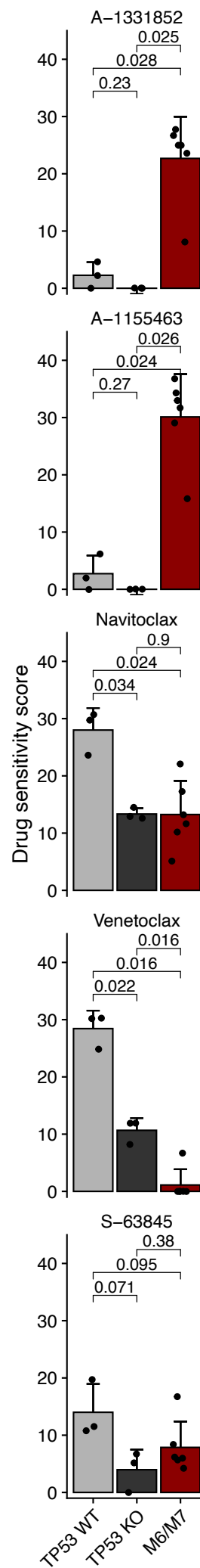
(D) Expression Z-scores of all measured genes after knockdown of *GFI1B* or *GATA1* in K562 cells. *BCL2L1* and *GYPA* (encoding the erythroid differentiation marker glycophorin A) shown as reference are marked using red bars and labeled. Genes are ordered starting from lowest Z-score (indicating strongest downregulation following knockdown). Data are from genome-scale Perturb-seq experiments by Replogle et al.

Supplemental Figure 3

A



B



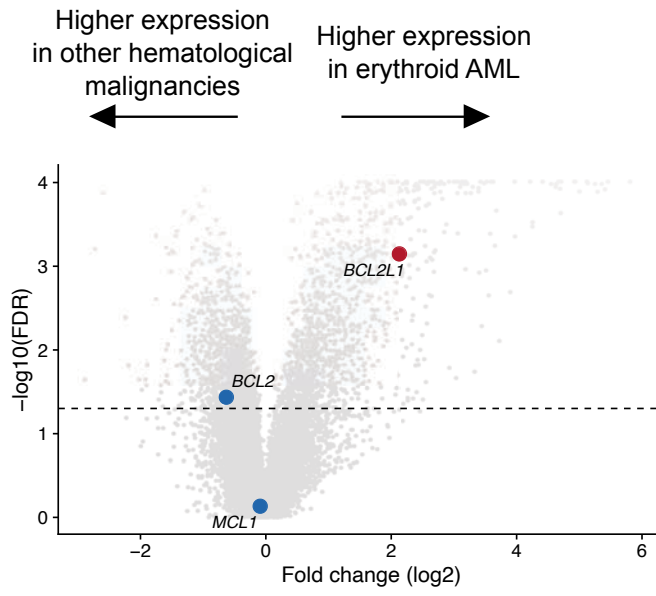
Supplemental Figure 3. Effect of *TP53* loss of function on BCL-2 family inhibitor sensitivity in AML.

(A) Bar plots comparing sensitivity of erythroid/megakaryocytic (M6/M7) and other AML cell lines both in *TP53* wild-type (left columns) and *TP53*-mutated (right columns) groups. *P* values were obtained using Wilcoxon rank sum tests. Bar heights indicate mean, error bars indicate standard deviation, and dots indicate individual cell lines.

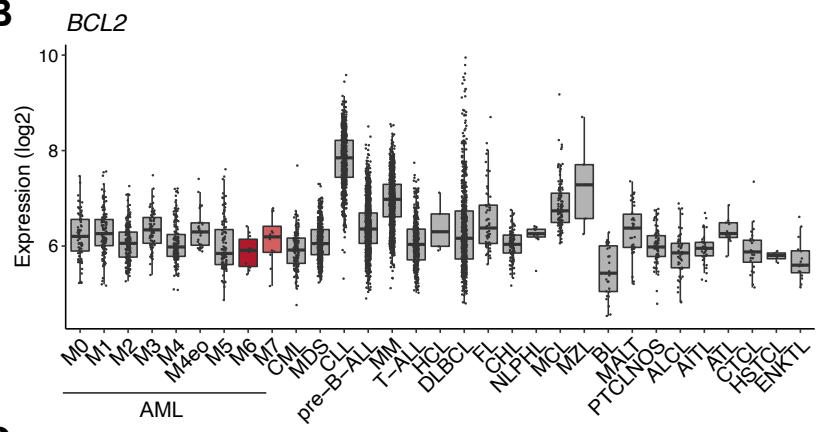
(B) Bar plots comparing drug sensitivities between CRISPR-mediated *TP53* knockout (KO) variants of the AML cell lines MOLM13, MV411, and OCIAML2 with the parental (WT) cell lines and with erythroid/megakaryocytic AML cell lines. *P* values between *TP53* KO and WT were obtained using paired Welch's *t*-test. *P* values between M6/M7 cell lines and *TP53* KO or WT and were obtained using Wilcoxon rank sum test. Bar heights indicate mean, error bars indicate standard deviation, and dots indicate individual cell lines.

Supplemental Figure 4

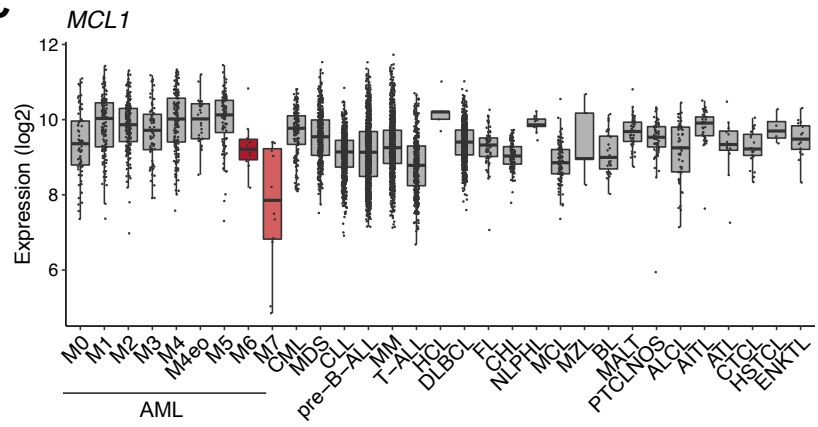
A



B



C



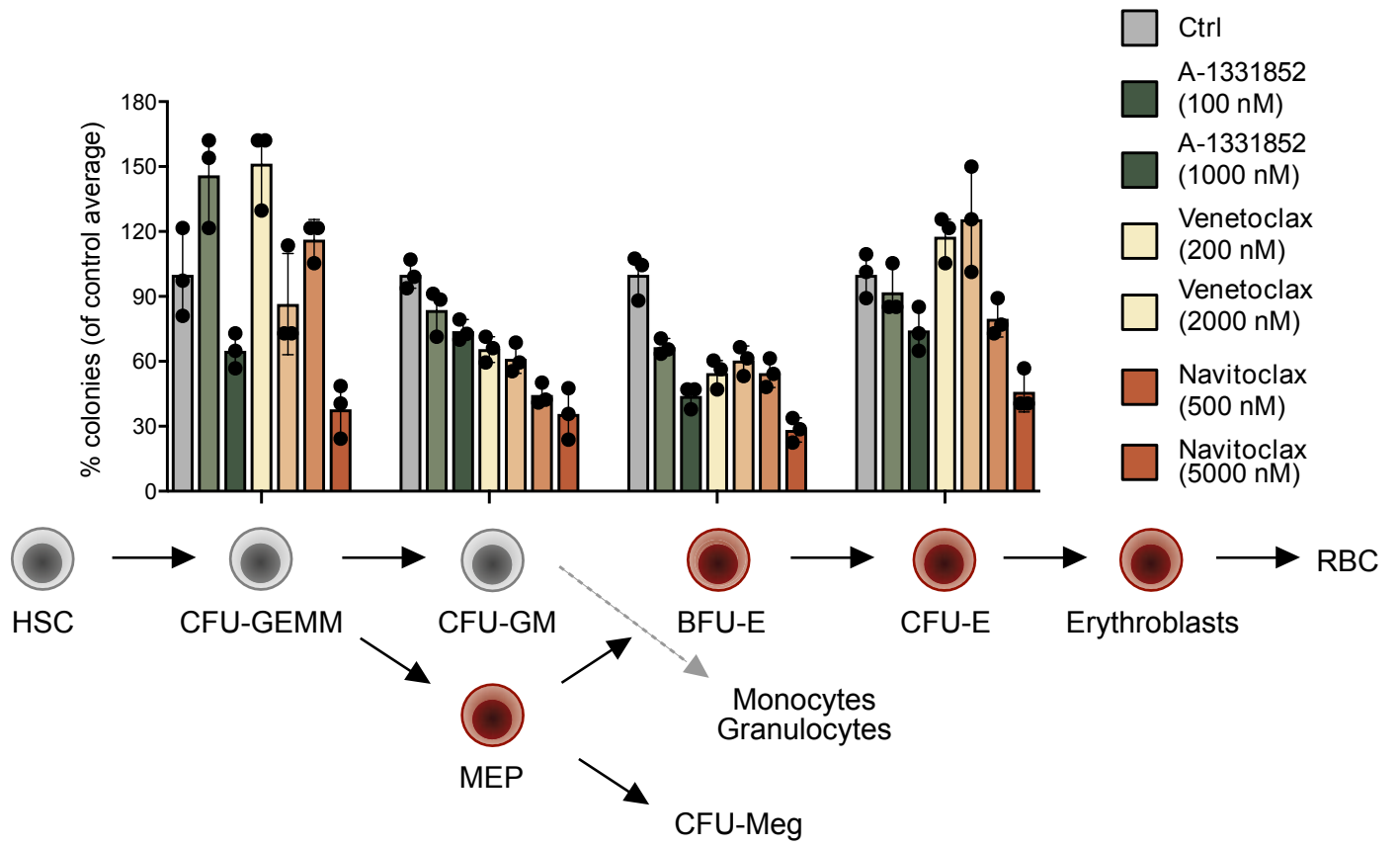
Supplemental Figure 4. Expression of *BCL2L1*, *BCL2*, and *MCL1* across hematological malignancies.

(A) Volcano plot of differential expression between AML M6 samples and all other hematological malignancies in the Hemap dataset using Wilcoxon rank-sum test. The BCL2 family genes *BCL2L1*, *BCL2*, and *MCL1* are labeled and colored based on the direction of the log₂ fold change.

(B) *BCL2* expression across hematological malignancies in the Hemap dataset.

(C) *MCL1* expression across hematological malignancies in the Hemap dataset.

Supplemental Figure 5

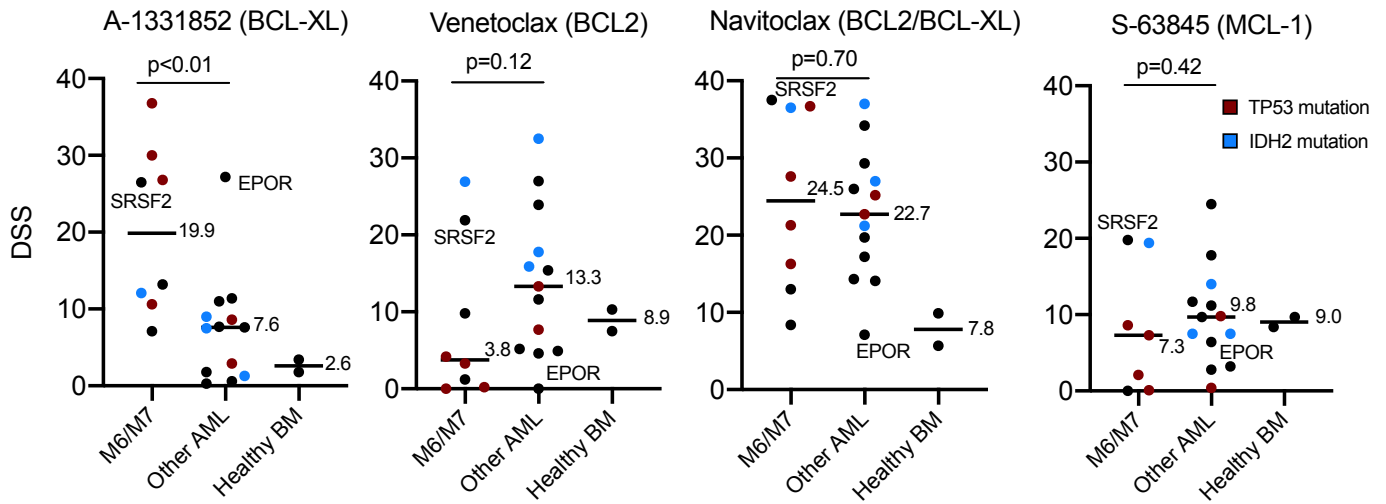


Supplemental Figure 5. Effects of BCL-2 family inhibitors on hematopoiesis in a colony-forming assay.

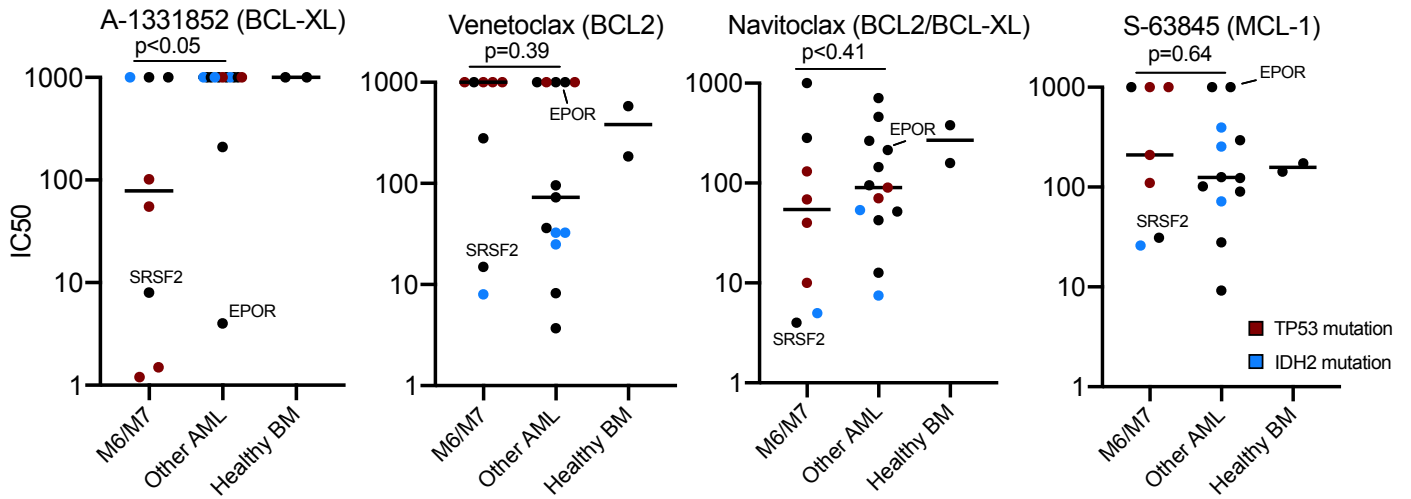
Colony forming potential of healthy bone marrow mononuclear cells under treatment with BCL-2 family inhibitors. Indicated compounds were added at two different concentrations in semi-solid medium and mixed with cells. Each dot represents a technical replicate and number of colonies were normalized to control after culturing the cells for 2 weeks. Bar heights indicate mean and error bars indicate range.

Supplemental Figure 6

A



B



C



Supplemental Figure 6. Sensitivity of AML patient samples to BCL-2 family inhibitors.

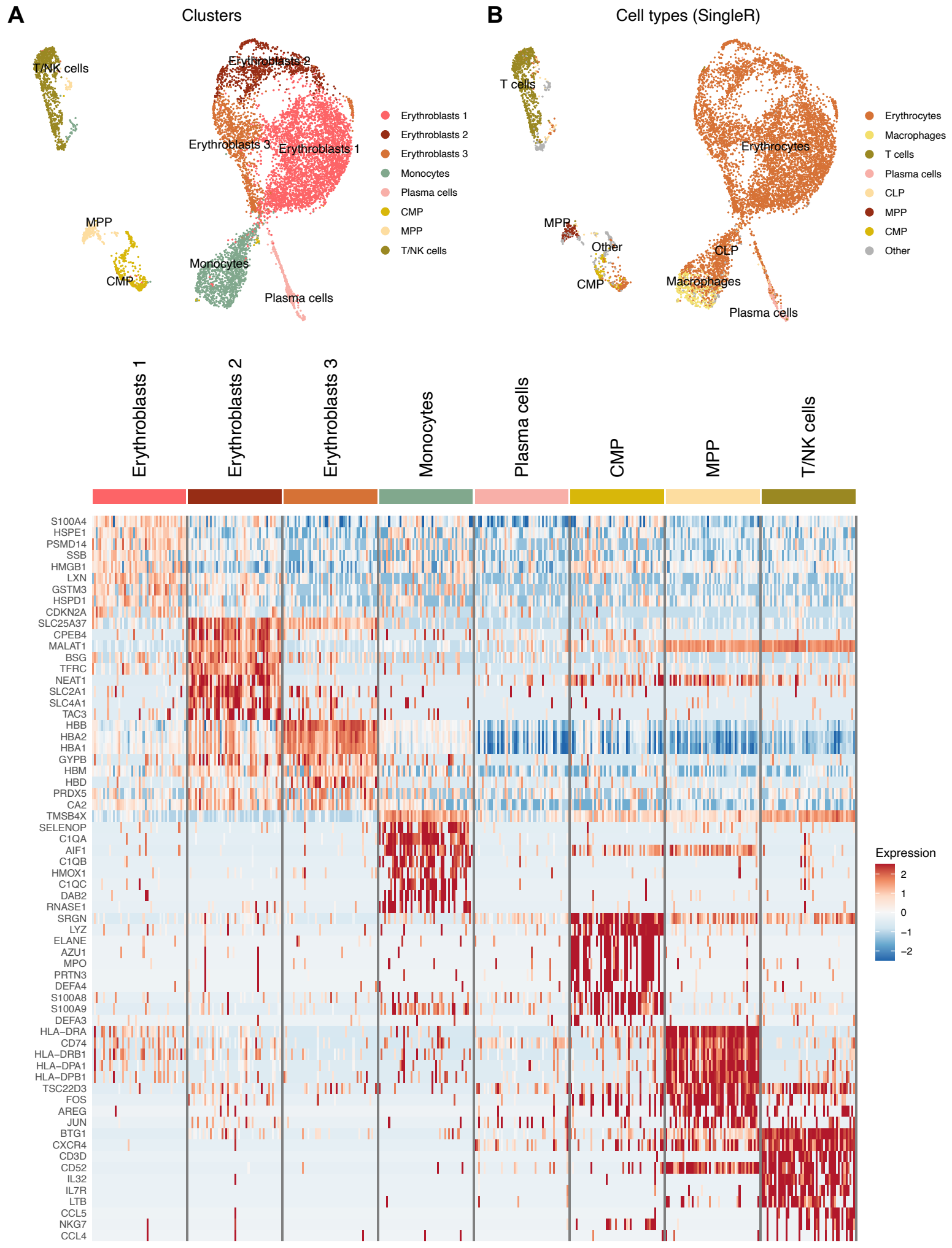
(A) *Ex vivo* drug sensitivity scores (DSS) of A-1331852, venetoclax, and navitoclax in AML patient samples (n = 21) and healthy bone marrow samples (n = 2). AML cases with *TP53* mutation are colored red, patients with *IDH2* mutation are colored blue and *SRFS2*, and *EPOR* mutations are labeled. P-values were calculated using the Wilcoxon rank sum test.

(B) IC50 values (absolute) of A-1331852, venetoclax, navitoclax, and S-63845 in AML patient samples (n = 21) and healthy bone marrow samples (n = 2).

(C) Location of the *EPOR* frameshift mutation shown in the *EPOR* protein. The R437Afs*8 frameshift leads to a stop codon at P443.

Supplemental Figure 7

AML with erythroid differentiation



Supplemental Figure 7. scRNA-seq of AML with erythroid differentiation.

(A) UMAP plot of scRNA-seq data of AML with erythroid differentiation (AML-5). Clusters identified using an unsupervised graph-based method are colored on the plot.

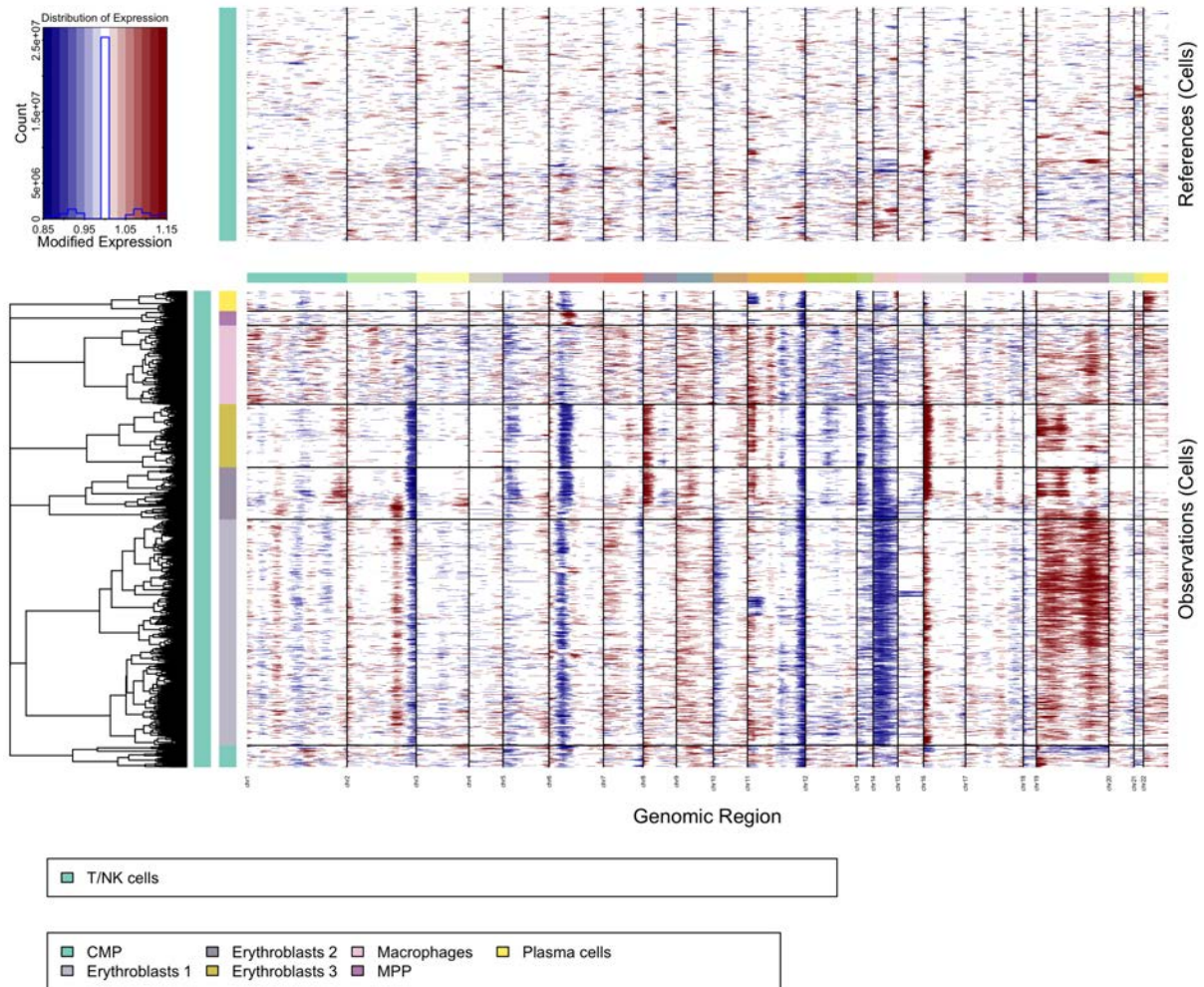
(B) UMAP as in A but with colors showing cell type annotations using the reference-based method SingleR.

(C) Heatmap showing most highly enriched genes in each cluster compared to other clusters.

Supplemental Figure 8

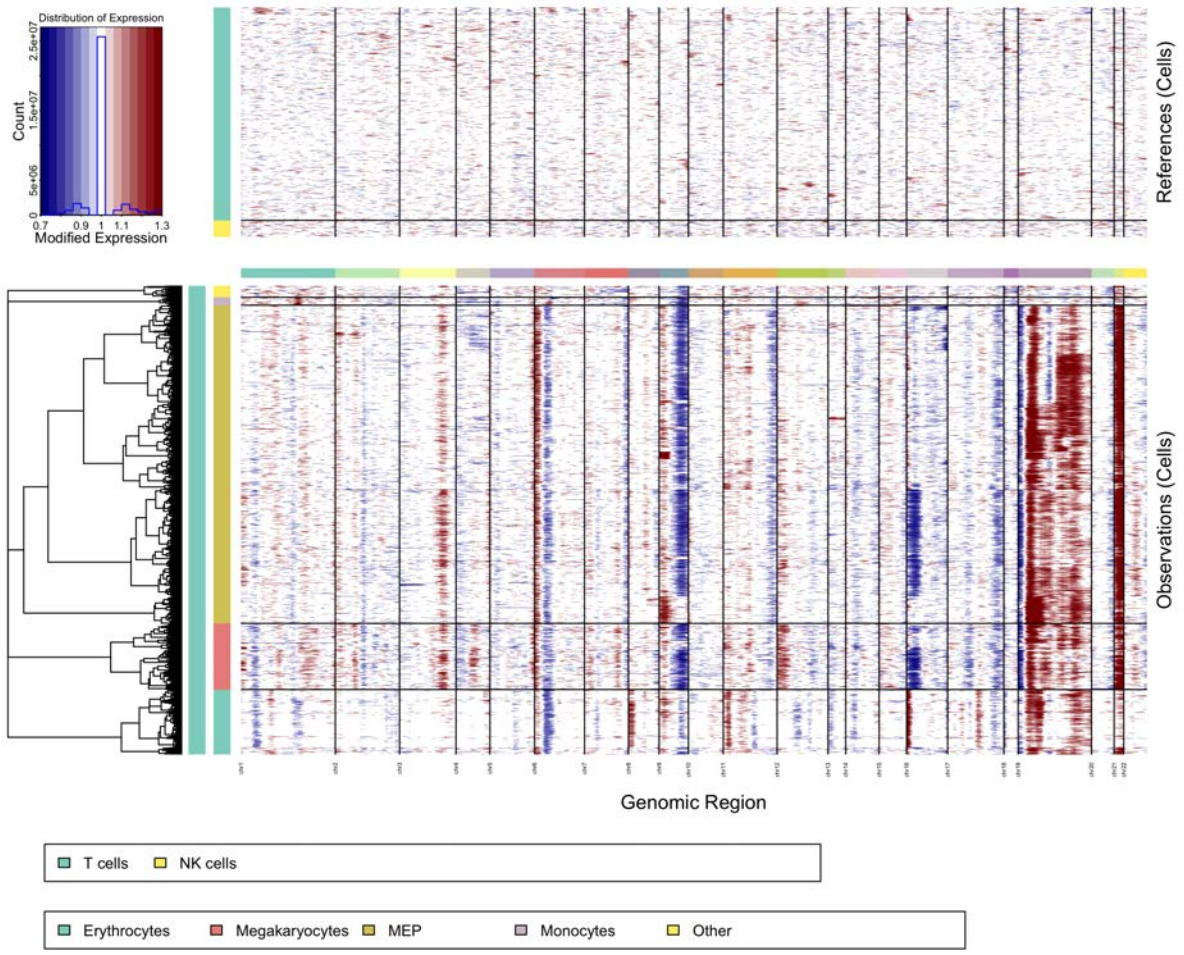
A

AML with erythroid differentiation



B

AML with megakaryocytic differentiation



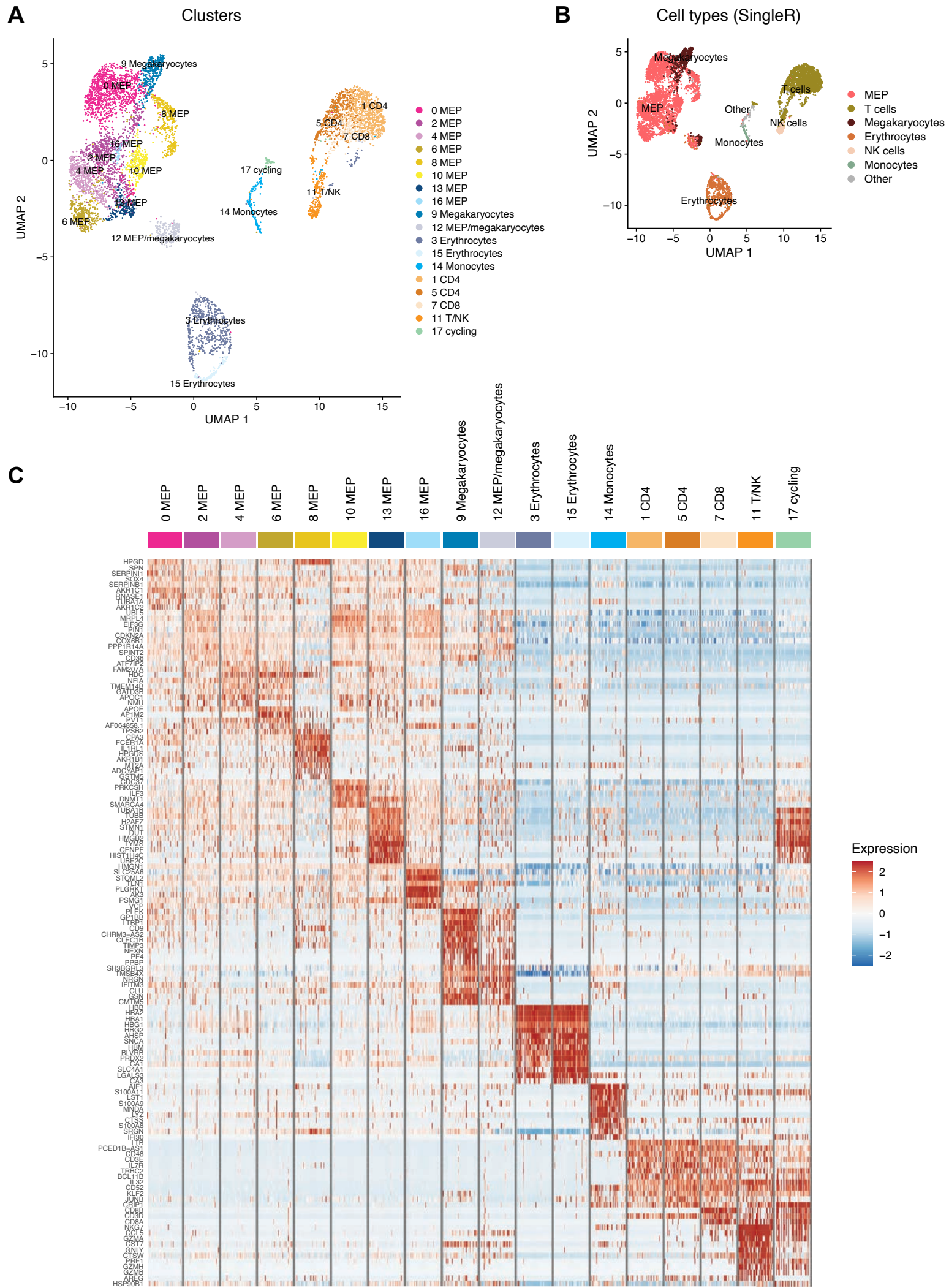
Supplemental Figure 8. Inference of copy-number alterations in scRNA-seq for identification of malignant cells.

(A) Heatmap showing expression levels of different genomic regions in either T and NK cells (used as normal reference) or in other cell types in scRNA-seq of the AML patients with erythroid differentiation (AML-5) produced using inferCNV. The rows indicate single cells grouped based on the cell type annotations and hierarchical clustering, and columns indicate different chromosomal regions. The graph shows similar copy-number alterations (CNAs) in the clusters Erythroblasts 1, 2, and 3, suggesting that they belong to the malignant population, whereas similar CNAs are not found in the Macrophages, Plasma cells, MPP, CMP, T and NK cells, suggesting that they represent normal cell types.

(B) Heatmap as in A for the AML patient with megakaryocytic differentiation (AML-1) produced using inferCNV. The graph shows similar CNAs in the Megakaryocytes and MEP, suggesting that they belong to the malignant population, whereas similar CNAs are not found in Monocytes, T and NK cells, and mostly in Erythrocytes, suggesting that they represent normal cell types.

Supplemental Figure 9

AML with megakaryocytic differentiation



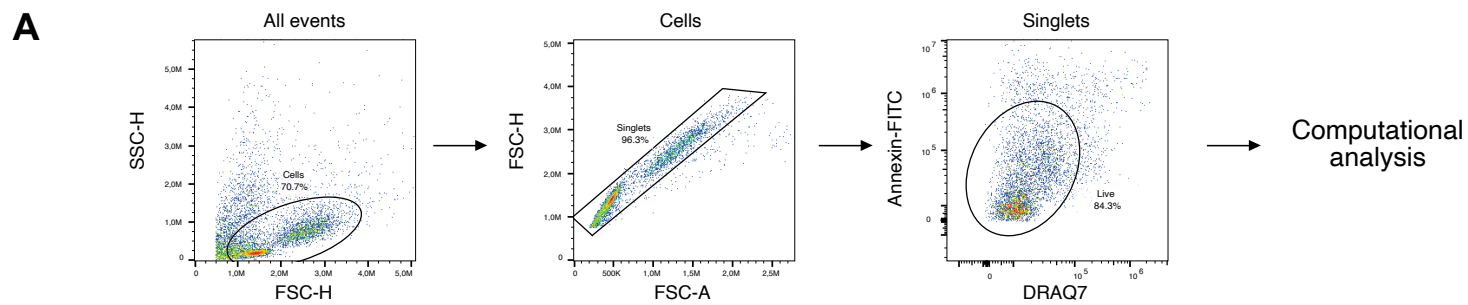
Supplemental Figure 9. scRNA-seq of AML with megakaryocytic differentiation.

(A) UMAP plot of scRNA-seq data of AML with megakaryocytic differentiation (AML-1). Clusters identified using an unsupervised graph-based method are colored on the plot.

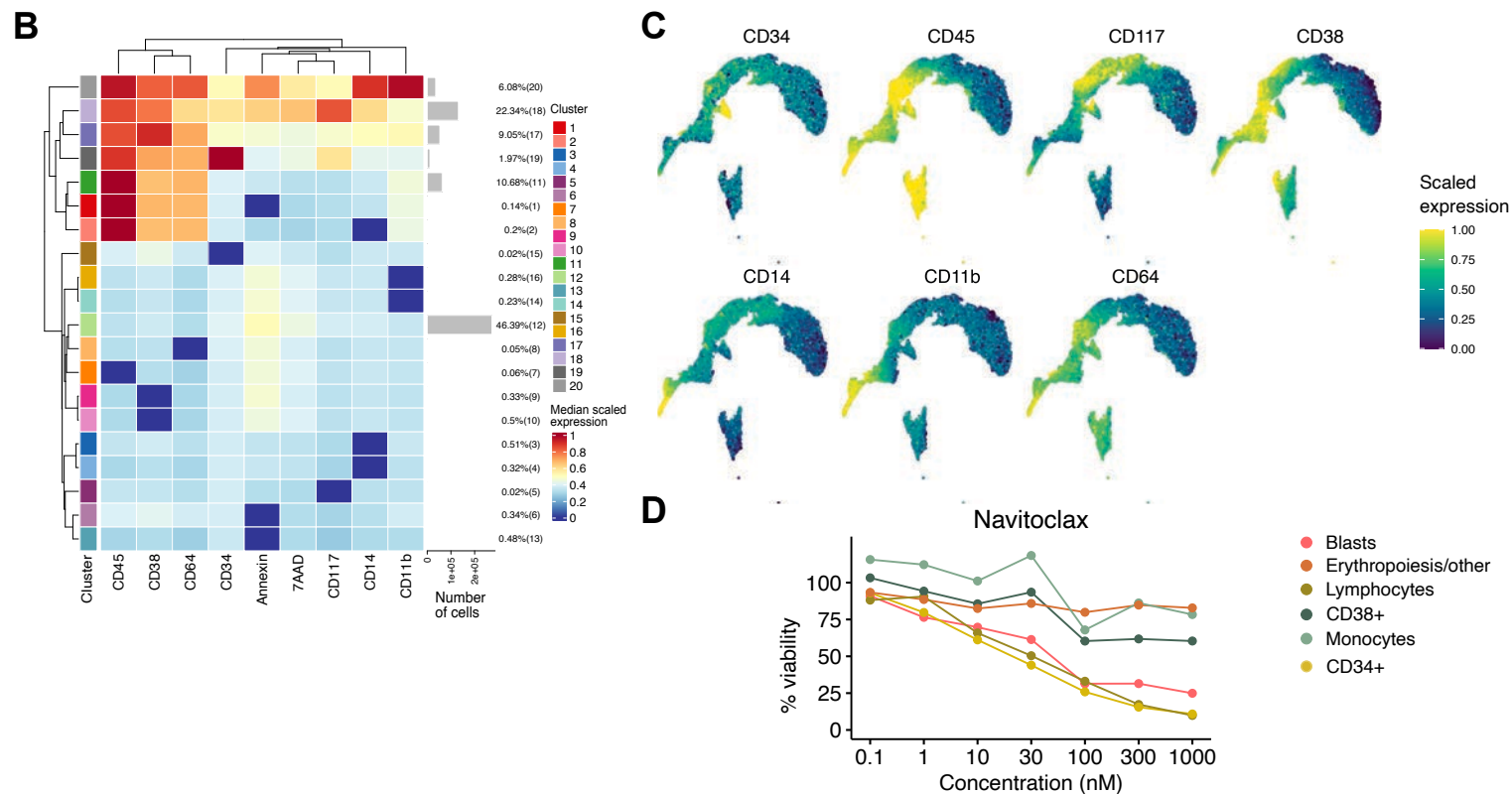
(B) UMAP as in A but with colors showing cell type annotations using the reference-based method SingleR.

(C) Heatmap showing most highly enriched genes in each cluster compared to other clusters.

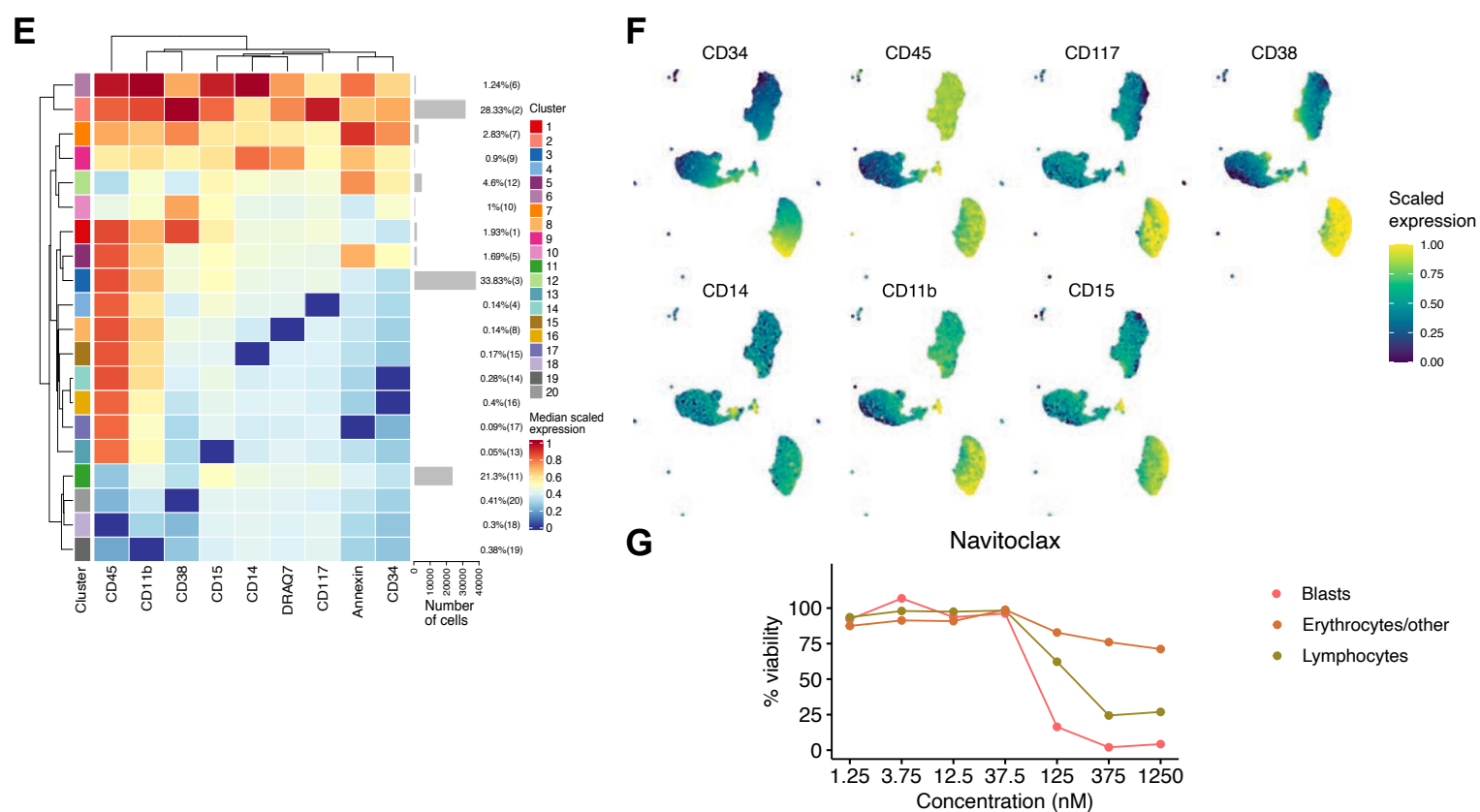
Supplemental Figure 10



AML with erythroid differentiation



AML with megakaryocytic differentiation



Supplemental Figure 10. Phenotype-based drug profiling using flow cytometry.

(A) Flow cytometry gating strategy to include viable single cells prior to computational unsupervised clustering analysis.

(B) Heatmap of median scaled expression of all surface markers across clusters identified by the FlowSOM method in cells of the AML patient with erythroid differentiation (AML-5). Clusters 2, 3, and 11 were retained in the drug sensitivity analysis as blasts, lymphocytes, and erythrocytes, respectively.

(C) UMAP plots showing scaled expression intensity of the indicated surface markers in cells of the AML patient with erythroid differentiation (AML-5).

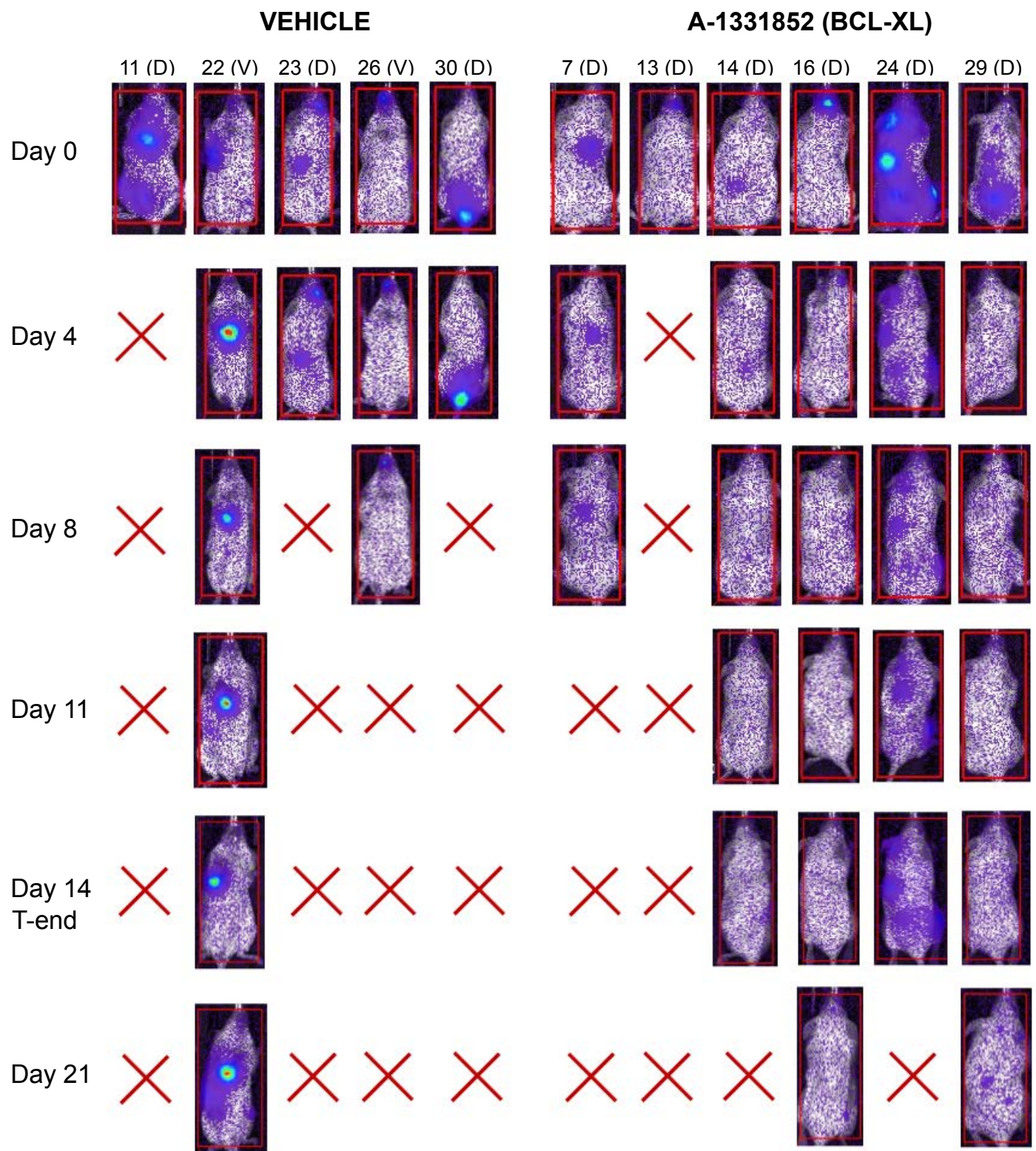
(D) Viabilities (percentage of viable cells compared to DMSO control) of the clusters representing different cell types in the AML patient with erythroid differentiation (AML-5) after treatment with indicated concentrations of navitoclax analyzed using flow cytometry-based drug profiling.

(E) Heatmap of median scaled expression of all surface markers across clusters identified by the FlowSOM method in cells of the AML patient with megakaryocytic differentiation (AML-1). Clusters 2, 3, and 11 were retained in the drug sensitivity analysis as blasts, lymphocytes and erythropoiesis/other, respectively.

(F) UMAP plots showing scaled expression intensity of the indicated surface markers in cells of the AML patient with megakaryocytic differentiation (AML-1).

(G) Viabilities (percentage of viable cells compared to DMSO control) of the clusters representing different cell types in the AML patient with megakaryocytic differentiation (AML-1) after treatment with indicated concentrations of navitoclax analyzed using flow cytometry-based drug profiling.

Supplemental Figure 11

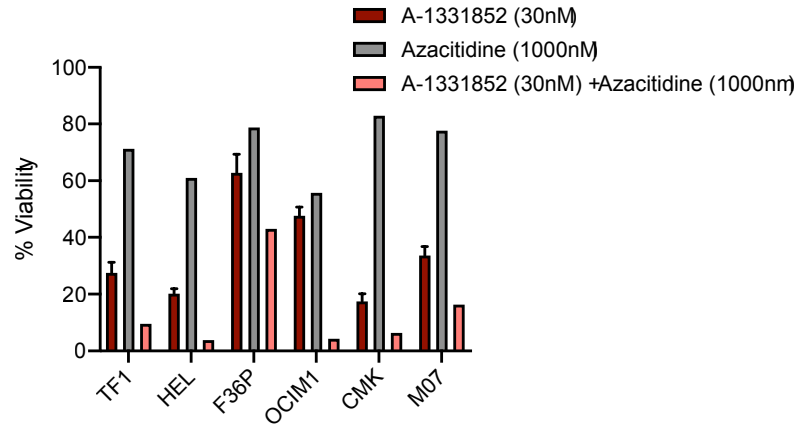


Supplemental Figure 11. Bioluminescence images of the xenograft mouse model.

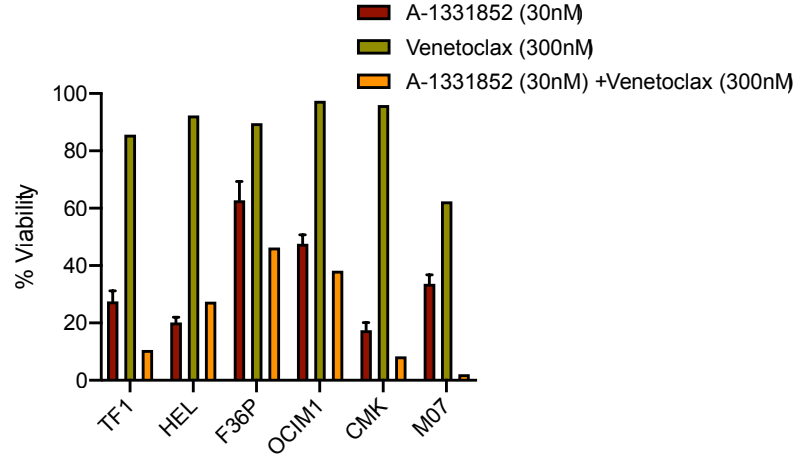
Eleven female NOD-SCID mice engrafted with luciferase-expressing HEL cells were treated orally with A-1331852 (25mg/kg, n=6) or vehicle (n=5) twice per day for two weeks. Tumor growth was measured with bioluminescence imaging using D-luciferin. Each column represents a dorsal or ventral side of an individual mouse (chosen based on higher signal) before start of the treatment (Day 0), during the two-week treatment period and one week after stopping the treatment. Red cross represents the time when a mouse either died or was euthanized due to poor condition.

Supplemental Figure 12

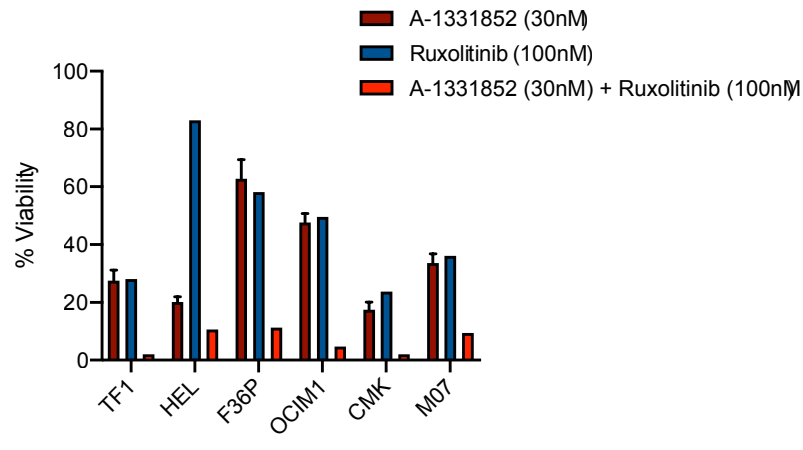
A



B



C



Supplemental Figure 12. Illustration of drug combination efficacy.

Efficacy of individual drugs and drug combinations on six erythroid and megakaryoblastic leukemia cell lines for the combinations of A-1331852 with azacitidine (A), venetoclax (B), and ruxolitinib (C). After 3 days of treatment, cell viability was measured using CellTiter-Glo. Bar plots illustrate cell viability at specific concentrations. A-1331852 efficacy was measured using 5 technical replicates with mean and standard deviation presented. For other compounds one measurement was used. The full concentration matrices are presented in supplemental Table 6.